DOI: 10.1002/chem.200601598

A General Strategy for the Rational Design of Size-Selective Mesoporous Catalysts

Clemens Zapilko, Yucang Liang, Willy Nerdal, and Reiner Anwander*[a]

Abstract: A series of functionalized mesoporous silicas with cagelike pore topology has been synthesized and screened for size-selective catalytic transformations. The aluminum-catalyzed Meerwein–Ponndorf–Verley (MPV) reduction of differently sized aromatic aldehydes (benzaldehyde and 1-pyrenecarbox-aldehyde) has been investigated as a test reaction. The catalysts were synthesized in a two-step grafting sequence comprising pore-size engineering of mesoporous silicas (SBA-1, SBA-2, SBA-16) with long-chain alkyl dimethylaminosilanes and surface organoaluminum chemistry with triethylaluminum [{Al-$(CH_2CH_3)_3\}_2$]. Size-selective reaction behavior was found for small pore SBA-1 materials, and the selectivity could be efficiently tuned by selecting a silylating reagent of appropriate size. The results are compared with the catalytic performance of a large-pore periodic mesoporous organosilica PMO-[SBA-1] and the nonporous high-surface-area silicas Aerosil 300/380.

Keywords: aluminum grafting · Meerwein–Ponndorf–Verley reduction · mesoporous materials · pore-size engineering · size selectivity

Introduction

Zeolites and related materials such as alumino- or gallophosphates[1] and periodic mesoporous silicas (PMSs),[2] mesoporous organosilicas (PMOs)[3] and mesoporous metal oxides[4] are ubiquitous inorganic porous high-surface-area materials that are widely used as catalyst supports both in industry and academic research. Zeolites and zeotypes are microporous materials (pore diameter < 2 nm), whereas PMSs and PMOs exhibit pore diameters in the range of 2 to 50 nm. Zeolites are crystalline substances with an atomic scale periodic ordering. In contrast, PMSs are considered semicrystalline with a periodic pore arrangement but with amorphous pore walls. Size- or shape-selective reactions, that is the preferred or exclusive transformation of a molecule that fits into the porous framework, are a unique and formidable phenomenon occurring in zeolitic materials.[5–7] A similar behavior of mesoporous materials has scarcely been observed until now. Among the few reports about shape selectivity dealing with non-zeolitic materials are catalytic reactions or adsorption experiments with pillared clays,[8] metal–organic frameworks,[9] or supramolecular assemblies.[10] Kishna et al. demonstrated the shape-selective synthesis of calix[4]pyrrols over a Lewis acidic MCM-41 catalyst.[11] The tailoring of mesoporous materials for size-selective adsorption and drug delivery has found widespread interest.[12] Some mesoporous materials (e.g. SBA-16) have pores too small to accommodate enzymes and display size selectivity in this respect.[13]

The PMS family includes materials with various pore configurations such as one-dimensional linear (MCM-41[2] and SBA-15[16]) or three-dimensional interconnected channel systems (MCM-48)[2] as well as cagelike pore structures. SBA-1,[17] SBA-2,[18] and SBA-16[19] are prominent examples for the latter type of materials being composed of nanosized cages, which are interconnected by smaller windows. These structural features resemble very much the structure of zeolites such as faujasite ($d_{supercage} = 1.3$ nm), but on a larger length scale, as the cages in SBA-1 and SBA-2 are typically 3–4 nm[20] in diameter and 4.5–9 nm in SBA-16.[21] The diameter of the interconnecting windows, however, can reach molecular dimensions, which is known from adsorption experiments with differently sized hydrocarbons[22] and from surface silylation reactions.[23] The detailed pore structure of these cagelike mesoporous materials has been elucidated by using electron crystallography and HRTEM techniques. SBA-2[24] and SBA-16[25] display a hexagonal close packing and a body-centered cubic array of supercages, respectively. SBA-1 and the isostructural organosilica PMO[SBA-1] fea-

[a] C. Zapilko, Dr. Y. Liang, Dr. W. Nerdal, Prof. Dr. R. Anwander
Kjemisk Institutt, Universitetet i Bergen
Allégaten 41, 5007 Bergen (Norway)
Fax: (+47) 555-89490
E-mail: reiner.anwander@kj.uib.no.

Supporting information for this article is available on the WWW under http://www.chemeurj.org/ or from the author.

ture a more complicated pore topology consisting of two differently sized ellipsoidal cages A and B which form an A_2B framework.[20] A cages are slightly larger than B cages ($d_A/d_B \approx 1.1$) and therefore different types of interconnecting windows (between two neighboring A cages and between A and B cages) are present in the structure. Owing to the amorphous pore walls, a pore-size distribution both of cages and windows has to be taken into account.[26]

Herein, we present a method for the preparation of size-selective mesoporous organic–inorganic hybrid catalysts. Our approach allows the rational design of selective catalysts following a simple building blocks principle, which comprises a mesoporous silica with a cagelike pore structure, a silylating reagent, and a catalytically active component, which can be a metal compound or an organic group, that is grafted onto the pore walls of the silica. Size selectivity is demonstrated for the Meerwein–Ponndorf–Verley (MPV) reduction of aromatic aldehydes to alcohols (Scheme 1).[4,15]

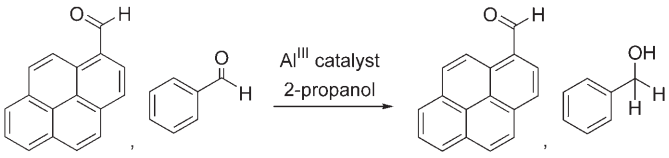

Scheme 1. MPV reduction of 1-pyrenecarboxaldehyde and benzaldehyde.

The MPV hydride-transfer reaction is routinely employed in organic synthesis and catalyzed by Lewis acidic aluminum,[15] magnesium,[27] or rare-earth metal isopropoxides.[28] 2-Propanol is used as solvent and as the reducing agent. The MPV reduction is an equilibrium reaction and therefore excess of 2-propanol is necessary to force the formation of the desired alcohol. Though the conversion is very selective and tolerant towards most functional groups, the aldol and the Tishchenko reaction may occur as side reactions.[14] The formation of aldol products can be suppressed if a metal alkoxide with a low Brønsted basicity is employed. In most cases aluminum isopropoxide is the catalyst of choice. Several heterogeneously promoted versions of the MPV reduction have been developed, which exploit, for example, magnesium oxide[29] and hydrotalcite as catalysts.[30] Grafting of aluminum isopropoxide onto mesoporous silica MCM-41 afforded a catalyst that shows a great acceleration of the reaction rate for the industrially important reduction of 4-*tert*-butylcyclohexanone to 4-tert-butylcyclohexanol compared to the homogeneous catalyst.[31]

Results and Discussion

Synthesis of cagelike mesoporous silicas and organosilicas: SBA-1,[32] SBA-2,[22] and SBA-16[21] were synthesized according to literature procedures, by employing octadecyltriethylammonium bromide, *N*-(3-trimethylammoniumpropyl)hexadecyldimethylammonium bromide, and Pluronic F127 poly(ethylene oxide)-poly(propylene oxide)-poly(ethylene oxide) triblock copolymer ($EO_{106}PO_{70}EO_{106}$) as structure-directing agents (SDAs), respectively. Tetraethylorthosilicate TEOS was used as a silica source. The as-synthesized materials were calcined at 540 °C and dehydrated in high vacuum to remove the organic template and physisorbed water. This treatment results in high-surface-area materials with specific Brunauer–Emmett–Teller (BET) surfaces a_s in the range of 680 to 1520 $m^2 g^{-1}$ and specific pore volumes V_p from 0.5 (SBA-16) to 0.81 $cm^3 g^{-1}$ (SBA-1) as determined from nitrogen physisorption measurements (for complete textural properties of parent and hybrid mesoporous silicas see Table 1). The organosilica PMO[SBA-1] was synthesized with octadecyltrimethylammonium bromide (C_{18}TABr) and *N*-(3-trimethylammoniumpropyl)octadecyldimethylammonium bromide ($C_{18\text{-}3\text{-}1}$) as structure-directing agents and 1,2-bis(triethoxysilyl)ethane (BTEE) as source of the organosilica framework.[33] The SDA was removed from the as-synthesized material by extensive Soxhlet extraction with hydrochloride-acidified ethanol, because the material can not withstand a calcination. A lower limit for the diameter of interconnecting channels and windows in the PMO[SBA-1]

Table 1. Textural properties and elemental analysis of pure silica materials and related hybrid materials.

Sample[a]	$a_{s,BET}$[b] [$m^2 g^{-1}$]	V_p[c] [$cm^3 g^{-1}$]	d_p[d] [nm]	C [wt %]	H [wt %]	Al [wt %]
SBA-1	1390	0.81	2.2			
PMO[SBA-1]	830	0.91	3.2	16.51	3.39	
SBA-2	940	0.69	2.5			
SBA-16	680	0.50	3.7			
$SiMe_2C_8H_{17}$@SBA-1	1200	0.52	1.5	18.98	4.30	
$SiMe_2C_{18}H_{37}$@SBA-1	< 10	< 0.01		22.40	4.46	
$SiMe_2C_8H_{17}$@SBA-16	360	0.27	3.6	9.43	2.28	
$SiMe_2C_{18}H_{37}$@SBA-16	10	0.01		13.2	2.57	
$AlEt_x$@PMO[SBA-1]	490	0.45	2.9	24.76	4.83	4.7
$AlEt_x$@SBA-1	630	0.26	1.6	17.99	3.66	8.4
$AlEt_x$@SBA-2	940	0.67	2.6	1.52	0.68	0.6
$AlEt_x$@SBA-16	320	0.23	3.6	7.95	1.75	4.7
$AlEt_x$@Aerosil380				9.44	1.98	5.2
$AlEt_x$@$SiMe_2C_8H_{17}$@SBA-1	490	0.20	1.4	21.28	4.29	5.6
$AlEt_x$@$SiMe_2C_{18}H_{37}$@SBA-1	< 10	< 0.01		24.99	4.81	1.6
$AlEt_x$@$SiMe_2C_8H_{17}$@SBA-16	170	0.14	3.5	10.2	2.37	3.1
$AlEt_x$@$SiMe_2C_{18}H_{37}$@SBA-16	10	0.01		14.1	2.65	0.3
$AlEt_x$@$SiMe_2C_8H_{17}$@Aerosil300				5.71	1.33	1.9
$AlEt_x$@$SiMe_2C_{18}H_{37}$@Aerosil300				7.72	1.72	2.0

[a] Pretreatment conditions: 250 °C (pure silica materials)/100 °C (silylated and metalated materials), 2.5 h, 10^{-3} Torr. [b] Specific BET surface area. [c] Total pore volume. [d] Pore diameter according to the maximum of the BJH pore size distribution calculated from the desorption branch.

structure is given by the kinetic diameter of the SDA molecules which diffuse through the internal pore volume during the extraction process. A BJH analysis of the nitrogen physisorption data shows a significantly larger pore diameter of PMO[SBA-1] (3.2 nm) compared with that of the pure silica SBA-1 (2.2 nm). From a chemical point of view, replacing a siloxane bridge in SBA-1 by a $\equiv Si(CH_2CH_2)Si\equiv$ moiety (in PMO[SBA-1]) renders the material more hydrophobic and reduces the density of reactive surface silanol groups ≡Si-OH.

Synthesis of organic–inorganic hybrid catalysts: The cagelike mesoporous silicas were allowed to react with solutions of excess triethylaluminum [$\{Al(CH_2CH_3)_3\}_2$] in hexane to form a set of aluminum-grafted hybrid materials. The reactions were conducted overnight at ambient temperature and monitored by FTIR spectroscopy. The peculiar band of the OH stretching vibration at 3695 cm^{-1} disappeared, indicating a complete consumption of all surface silanol groups ≡Si-OH in SBA-1, SBA-16, and PMO[SBA-1] by the highly reactive aluminum alkyl. The resulting grafted materials are denoted $AlEt_x$@SBA-1, $AlEt_x$@SBA-16, and $AlEt_x$@PMO-[SBA-1]. The transformation liberates ethane and establishes stable Al-O-Si linkages. The grafted aluminum centers exhibit a highly distorted and unsaturated coordination sphere, which imparts strong Lewis acidity and remarkable activity in catalytic MPV reductions. For SBA-2 the grafting reaction does not proceed to completeness. A significant number of nonreacted ≡Si-OH groups are still visible in the IR spectrum. The amount of aluminum found in $AlEt_x$@SBA-2 is as low as 0.6 wt% compared to 8.4 and 4.7 wt% in completely grafted $AlEt_x$@SBA-1/16 (Table 1). We assume that the triethylaluminum cannot pass the small windows of the porous structure of SBA-2, indicating the feasibility of size-selective reactions with this kind of cagelike mesoporous materials. Nitrogen physisorption measurements revealed the expected decrease of pore volume, specific surface area, and pore diameter for the grafted materials (Figure 1, Table 1).

While the maximum of the BJH pore-size distribution of $AlEt_x$@SBA-16 is still clearly in the range of mesopores (3.6 nm), the pores of $AlEt_x$@SBA-1 are confined to the microporous range (1.6 nm). SBA-1 features a type IV isotherm, typical for mesoporous materials, with a steep capillary condensation step at a relative pressure $P/P_0 = 0.2$. Upon the grafting procedure this isotherm developed into a type I isotherm indicative of a microporous material.

As organic fine chemicals are usually smaller than 1.6 nm, and the BJH method tends to underestimate the true pore extensions, we rationalized that size-selective catalysis might require materials with even smaller pore diameters. These materials could be obtained by immobilizing bulky organic groups onto the materials surface. Therefore, a two-step consecutive grafting procedure was established, which consists of a silylation experiment and a subsequent metalation step. Dimethylaminosilanes (Me_2NSiMe_2R) with differently sized alkyl chains, dimethyl(dimethylamido)octylsilane, and

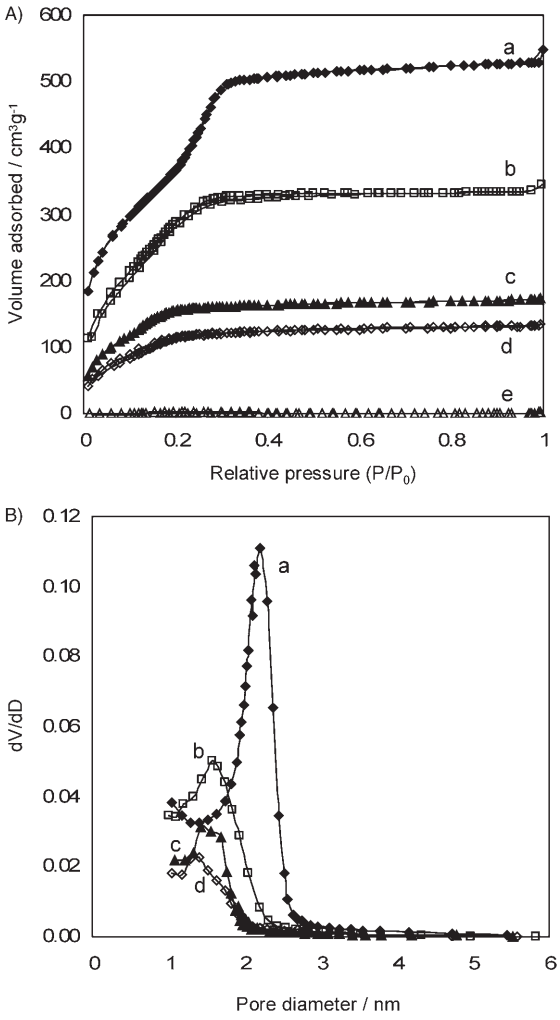

Figure 1. Nitrogen phyisisorption isotherms (A) and corresponding BJH pore-size distributions (B) of SBA-1 (a) and hybrid materials $SiMe_2C_8H_{17}$@SBA-1 (b), $AlEt_x$@SBA-1 (c), $AlEt_x$@ $SiMe_2C_8H_{17}$@SBA-1 (d), and $SiMe_2C_{18}H_{37}$@SBA-1 (e).

dimethyl(dimethylamido)octadecylsilane were employed in the silylation experiment.[34] These monosilazane compounds are known to react rapidly with dehydrated silica surfaces at ambient temperature and are in this respect advantageous compared to the routinely used chloro- or alkoxysilanes, which require elevated temperatures or basic auxiliaries.[35] The amount of the silylating reagent was chosen to be 30% of the chemically accessible SiOH groups. Thus, the majority of the reactive surface functionalities remain unchanged by the silylation procedure. Owing to the high reactivity of the dimethylaminosilanes, the silylation proceeds rapidly and it is likely that mainly silanol groups located at the external surface of the silica particles and the pore openings are derivatized. Accordingly, the pre-functionalization ensures passivation of the external particle surface and concomitant tailoring of the free diameter of the pore openings dependent on the length of the grafted alkyl chain.

This methodology is based on work of Kruk et al., which was concerned with the functionalization of SBA-16 materi-

als with chlorosilanes.[36] For SBA-1-derived hybrid materials, we achieved a gradual decrease of the pore diameter from 2.2 nm (SBA-1) over 1.5 nm ($SiMe_2C_8H_{17}$@SBA-1) to complete blocking of the pore entrances ($SiMe_2C_{18}H_{37}$@SBA-1, Table 1 and Figure 1). Consequently, the detectable specific pore volume decreases in the same direction and vanishes ($<0.01\ cm^3g^{-1}$) for $SiMe_2C_{18}H_{37}$@SBA-1. For the silylated SBA-16 materials, a similar development of their textural properties was observed (Table 1, Supporting Information).

In a second preparation step, aluminum centers were grafted onto the intrapore silica surface by reacting the remaining silanol groups with triethylaluminum [{Al-$(CH_2CH_3)_3$}$_2$]. The resulting materials $AlEt_x$@$SiMe_2C_8H_{17}$@SBA-1/16 and $AlEt_x$@$SiMe_2C_{18}H_{37}$@SBA-1/16 show a lower amount of grafted aluminium centers compared to the non-silylated $AlEt_x$@SBA-1/16. This finding is in accordance with the reduced number of SiOH groups of the silylated materials. Interestingly, the surface silanol moieties of $SiMe_2C_{18}H_{37}$@SBA-1 and $SiMe_2C_{18}H_{37}$@SBA-16 are not fully accessible to triethylaluminum as indicated by FTIR spectroscopy (for representative IR spectra see Supporting Information). The more open porous structures of $SiMe_2C_8H_{17}$@SBA-1/16 react completely with [{Al-$(CH_2CH_3)_3$}$_2$]. Accordingly, size-selective behavior of these materials is already proposed by these distinct surface functionalizations.

NMR investigation of hybrid catalysts: ^{13}C MAS NMR spectra of the materials $SiMe_2C_8H_{17}$@SBA-1 and $AlEt_x$@$SiMe_2C_8H_{17}$@SBA-1 were recorded (Figure 2 A,B). $SiMe_2C_8H_{17}$@SBA-1 displays seven distinct signals for the octyldimethylsilyloxy groups.[35] Upon grafting of triethylaluminum, an additional signal appeared at about 8 ppm, which can be assigned to CH_3 moieties of aluminum-bound ethyl ligands. The signal of the methylene carbon atom of the CH_2CH_3 groups overlaps with the methyl signal of $SiMe_2C_8H_{17}$ units.[37] The catalytic MPV reduction is conducted in 2-propanol as a solvent, and therefore we stirred the precatalyst $AlEt_x$@$SiMe_2C_8H_{17}$@SBA-1 for 4 h in 2-propanol at ambient temperature. Under these conditions a ligand-exchange reaction occurs and ethyl ligands are replaced by isopropoxy moieties (Scheme 2). The resulting material Al(O*i*Pr)$_x$@$SiMe_2C_8H_{17}$@SBA-1 was filtered off, dried under vacuum, and a ^{13}C MAS NMR spectrum was recorded (Figure 2 C). Signals at $\delta = 68$ and 63 ppm (secondary carbon atoms) as well as $\delta = 27$ and 22 ppm (primary carbon atoms) document the presence of aluminum isopropoxide surface complexes.[38] Albeit showing a markedly decreased relative intensity, the ^{13}C resonance at about $\delta = 8$ ppm might be indicative of nonreacted $AlCH_2CH_3$ moieties or $SiCH_2CH_3$ groups formed by siloxane cleavage during the $AlEt_3$-grafting.[39]

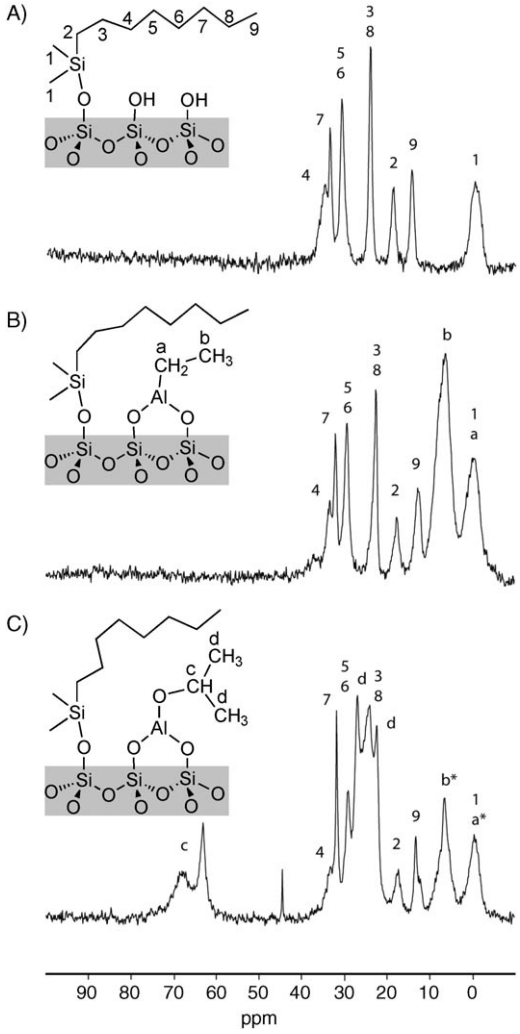

Figure 2. ^{13}C MAS NMR spectra of A) $SiMe_2C_8H_{17}$@SBA-1, B) $AlEt_x$@$SiMe_2C_8H_{17}$@SBA-1, and C) Al(O*i*Pr)$_x$@$SiMe_2C_8H_{17}$@SBA-1 and schematic drawings of proposed surface species.

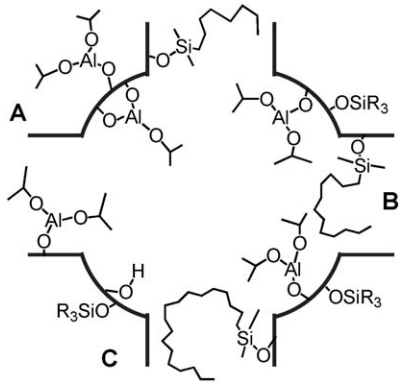

Scheme 2. Schematic representation of the cagelike pore structure of hybrid catalysts Al(O*i*Pr)$_x$@SBA-1 (**A**), Al(O*i*Pr)$_x$@$SiMe_2C_8H_{17}$@SBA-1 (**B**), and Al(O*i*Pr)$_x$@$SiMe_2C_{18}H_{37}$@SBA-1 (**C**).

Catalytic MPV reduction: Table 2 lists the metalated and/or silylated mesoporous materials that were tested in the catalytic MPV reduction of aromatic aldehydes. In addition, we synthesized the nonporous materials $AlEt_x$@$SiMe_2C_8H_{17}$@Aerosil300, $AlEt_x$@$SiMe_2C_{18}H_{37}$@Aerosil300, and $AlEt_x$@Aerosil380. Aerosil300 and Aerosil380 are amorphous silica

Table 2. MPV reduction of benzaldehyde and 1-pyrenecarboxaldehyde over various hybrid catalysts.[a]

Catalyst precursor	Conversion benzaldehyde [%]	Conversion 1-pyrenecarboxaldehyde [%]
$AlEt_x$@Aerosil 380[b]	91(5)	87 (5)
$AlEt_x$@$SiMe_2C_8H_{17}$@Aerosil 300[b]	46 (7)	27 (7)
$AlEt_x$@$SiMe_2C_{18}H_{37}$@Aerosil 300[b]	43 (7)	36 (7)
$AlEt_x$@PMO[SBA-1][b]	56 (5)	60 (5)
$AlEt_x$@SBA-1[b]	92 (5)	38 (5)
$AlEt_x$@$SiMe_2C_8H_{17}$@SBA-1[b]	91 (5)	11 (5)
$AlEt_x$@$SiMe_2C_{18}H_{37}$@SBA-1[b]	62 (28)	3 (28)
$AlEt_x$@$SiMe_2C_8H_{17}$@SBA-16[c]	95 (5)	61 (5)
$AlEt_x$@SBA-2[c]	4 (24)	2 (24)
$AlEt_x$@SBA-2[b,d]	73 (24)	62 (24)

[a] Values in parenthesis give the time [h] after which the conversion was obtained. [b] The amount of catalyst was adjusted to 6.6×10^{-2} mmol Al. [c] 50 mg catalyst used. [d] Experiment conducted at 80 °C.

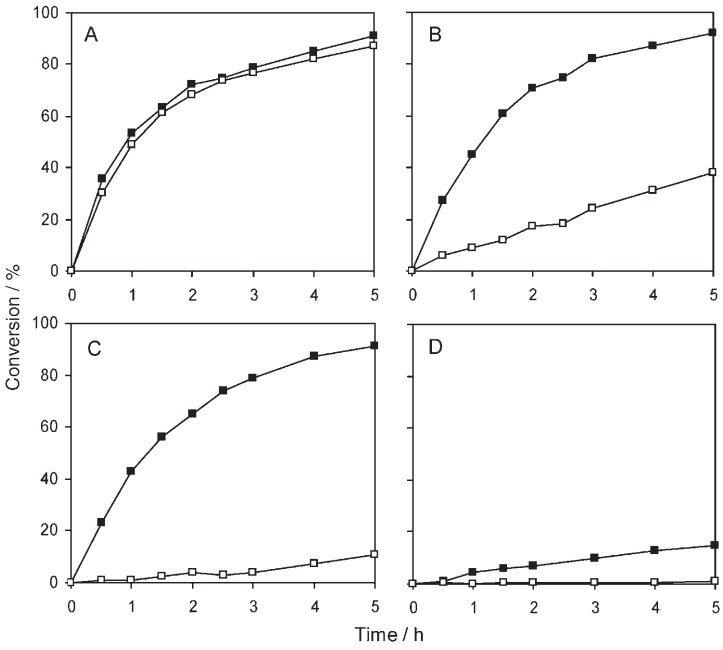

Figure 3. Conversion of benzaldehyde (■) and 1-pyrenecarboxaldehyde (□) in MPV reductions over various hybrid catalysts. A) $AlEt_x$@Aerosil 380, B) $AlEt_x$@SBA-1, C) $AlEt_x$@$SiMe_2C_8H_{17}$@ SBA-1, D) $AlEt_x$@ $SiMe_2C_{18}H_{37}$@ SBA-1.

materials with a BET surface area of about 300 and 380 m^2g^{-1}, respectively.

Two differently sized aromatic aldehydes, benzaldehyde and 1-pyrenecarboxaldehyde, were used as substrates in the catalytic MPV reduction (Scheme 1). The reactions were conducted at ambient temperature and the conversion of aldehyde was monitored by GC analysis versus dodecane as an internal standard. Aryl methanols were the sole detectable reaction products under these conditions. In each catalytic run, both aldehydes were added to the reaction mixture to probe the competition between a small and a large substrate molecule for access to the catalytically active metal centers.

Owing to their chemical similarity, benzaldehyde ($\varnothing \approx 0.92$ nm = van-der-Waals distance between carbonyl oxygen and the farthest hydrogen) and 1-pyrenecarboxaldehyde ($\varnothing \approx 1.29$ nm) showed similar reactivity toward nonporous $AlEt_x$@Aerosil380, $AlEt_x$@$SiMe_2C_8H_{17}$@Aerosil300, and $AlEt_x$@$SiMe_2C_{18}H_{37}$@Aerosil300 (Table 2, Figure 3A). These results clearly indicate that no preferred adsorption or molecular recognition of one of the substrates at the different catalyst surfaces occurs. Whereas the large-pore material $AlEt_x$@PMO[SBA-1] revealed also no substrate discrimination (Table 2 and Supporting Information), smaller pore sized $AlEt_x$@SBA-1 gave slightly different reaction rates with benzaldehyde being 4–6 times more reactive than 1-pyrenecarboxaldehyde (Table 2, Figure 3B). The hybrid catalyst $AlEt_x$@$SiMe_2C_8H_{17}$@SBA-1 revealed a slightly lower activity than the non-silylated materials, however, the relative reaction rate increased to 17:1 in favor of the smaller benzaldehyde. After 2 h, 65% of the benzaldehyde and only 4% of the 1-pyrenecarboxaldehyde were converted into the corresponding alcohols (Figure 3C). The activity of the hybrid catalyst is markedly reduced when the SBA-1 material is derivatized with a $C_{18}H_{37}$ alkyl chain. $AlEt_x$@ $SiMe_2C_{18}H_{37}$@SBA-1 gave only 15% conversion of benzaldehyde after 5 h. However, the size selectivity increased to a relative reaction rate of 20:1, resulting in quantitative formation of benzaldehyde but only 17% conversion of 1-pyrenecarboxaldehyde after four days (Figure 3D). As a result of these experiments we can state that the substrate selectivity of the heterogeneously performed MPV reduction can be efficiently tuned by selecting an appropriate support material; cagelike SBA-1 is superior to nonporous amorphous silica. Moreover, the same SBA-1 materials corroborate a beneficial effect of pore-size engineering by partial surface silylation with a monosilazane coupling reagent of suitable size.

$AlEt_x$@SBA-2 showed only very low activity in MPV reductions, in accordance with the low aluminum content of this material. At elevated temperature (80 °C), good conversion could be also achieved for the SBA-2 catalyst, albeit without selectivity (Table 2). We assume that most of the grafted aluminum species are located at the external surface of the SBA-2 particles and therefore cannot provide size selectivity. Significant size selectivity could also not be observed for the SBA-16 materials. Regardless the size of the silylating agent, the benzaldehyde and 1-pyrenecarboxaldehyde discrimination did not exceed a relative reaction rate of about 2.5:1 (Table 2 and Supporting Information). This discrepancy can certainly be rationalized on the basis of larger cage-interconnecting windows; however, clearly more knowledge has to be acquired about the nature of the pore openings and interconnecting channels in different cagelike PMSs.

Conclusion

We have established a new concept for accomplishing size selectivity in heterogeneous catalysis based on mesoporous silicas. Size-selective organic–inorganic hybrid catalysts can be obtained in a two-step consecutive grafting procedure. First, a mesoporous silica with a cagelike pore structure and a sufficiently small pore diameter (i.e. SBA-1) is selected and the pore size is tailored by grafting a bulky silylating reagent (i.e., dimethyl(dimethylamido)octylsilane) onto the silica surface. Second, a catalytically active metal compound is immobilized on the porous structure of the silica. The aluminum-grafted catalysts $AlEt_x@SiMe_2C_8H_{17}@SBA\text{-}1$ and $AlEt_x@SiMe_2C_{18}H_{37}@SBA\text{-}1$ exhibit good selectivity in discriminating between differently sized aldehydes, benzaldehyde and 1-pyrenecarboxaldehyde, in the Meerwein–Ponndorf–Verley reduction to alcohols. PMS SBA-1 seems to be a superior host material for the design of size-selective catalysts. There are virtually no restrictions for choosing a suitable metal compound and a silylating reagent from the large pool of already known grafting precursors. We synthesized a titanium-containing hybrid catalyst $Ti(NMe_2)_x@SiMe_2Ph@SBA\text{-}1$ following the procedure outlined above for the aluminum catalysts, by employing $(SiMe_2Ph)_2NH$ as a silylating reagent and tetrakis(dimethylamido)titanium $[Ti(NMe_2)_4]$ as a metal precursor. Preliminary investigations of an aminopropyl(triethoxy)silane (APS)-functionalized SBA-1 in the Knoevenagel condensation reaction of the above-mentioned aldehydes with ethylcyanoacetate show that this newly developed concept can be also applied in organocatalysis. These simple qualitative relations between the size of the silylating reagent and the selectivity observed for the resulting catalyst open up new possibilities for the rational design of shape-selective catalysts and adsorbents. We believe that this approach will broaden the scope of shape-selective reactions in fine chemical synthesis, and that functionalized cagelike mesoporous catalysts will prolifically complement the long-known zeolitic materials.

Experimental Section

Materials and methods: Tetraethylorthosilicate (TEOS) from Fluka was used as a silica precursor. Tetramethylammonium hydroxide (25 wt% solution in water, TMAOH), octadecyl bromide, hexadecyldimethylamine, triethylamine, 1,2-bis(triethoxysilyl)ethane, octadecyldimethylamine, octadecyltrimethylammonium bromide (C_{18}TABr), dimethyloctylchlorosilane, dimethyldodecylchlorosilane, dimethyloctadecylchlorosilane, triethylaluminum, dodecane, and (3-bromopropyl)trimethylammonium bromide were purchased from Aldrich. 1,1,3,3-Tetramethyldisilazane was obtained from Gelest, and Pluronic F127 poly(ethylene oxide)-poly(propylene oxide)-poly(ethylene oxide) triblock copolymer ($EO_{106}PO_{70}EO_{106}$) from Sigma. The reagents were used as received without further purification. Octadecyltriethylammonium bromide $[CH_3(CH_2)_{17}NEt_3]^+Br^-$ (C_{18}TEABr), *N*-(3-trimethylammoniumpropyl)hexadecylammonium dibromide $[CH_3(CH_2)_{15}NMe_2(CH_2)_3NMe_3]^{2+}2\,Br^-$ ($C_{16\text{-}3\text{-}1}$) and *N*-(3-trimethylammoniumpropyl)hexadecylammonium dibromide $[CH_3(CH_2)_{17}NMe_2(CH_2)_3NMe_3]^{2+}2\,Br^-$ ($C_{18\text{-}3\text{-}1}$) were synthesized according to literature procedures by reacting octadecyl bromide with triethylamine and hexadecyldimethylamine and octadecyldimethylamine with (3-bromopropyl)trimethylammonium bromide, respectively.[40] Aerosil300 and Aerosil380 were donated by Degussa AG. The PMS and PMO materials were synthesized according to slightly modified literature procedures. Grafting experiments and Meerwein–Ponndorf–Verley reductions were performed with rigorous exclusion of air and water, using high-vacuum and glovebox techniques (MBraun MB150B-G; <1 ppm O_2, <1 ppm H_2O). Solvents were purified by using Grubbs columns (MBraun SPS, solvent purification system). Calcined mesoporous silicas were dehydrated under high vacuum for 4 h at 270 °C. The catalytic reactions were monitored by gas chromatography, using a Hewlett Packard 5890 FID instrument equipped with an hp Ultra 1 column (crosslinked methyl siloxane, 25 m × 0.2 mm × 0.3 μm film thickness) versus dodecane as internal standard (temperature program: 50 °C initial temperature for 4 min; heating rate 15 °C min^{-1}; final temperature 220 °C for 15 min.

Powder X-ray diffraction (PXRD) patterns were recorded on a Philips X′pert PRO instrument in the step/scan mode (step width, 0.034; accumulation time, 30 s per step; range (2Θ), 0.31–9.96°) using monochromatic $Cu_{K\alpha}$ radiation ($\lambda = 1.5418$ Å). IR spectra of the parent and functionalized materials were recorded on a Perkin-Elmer Fourier transform infrared (FTIR) spectrometer 1760X using Nujol mulls sandwiched between CsI plates. The ^{13}C MAS NMR spectra were obtained at 125.76 MHz on a Bruker-BIOSPIN-AV500 instrument (5 mm BBO) equipped with *magic angle spinning* (MAS) hardware and using ZrO_2 rotors with a diameter of 4 mm. Experiments were done at a sample temperature of 298 K with a sample spinning rate of 10 kHz. The ^{13}C MAS NMR experiments on all three samples were carried out with high-power proton decoupling during the acquisition, that is without nuclear Overhauser effect (NOE) and a relaxation delay of 15 s between a total of 3800 transients for sample $SiMe_2C_8H_{17}@SBA\text{-}1$ and 4400 transients for samples $AlEt_x@SiMe_2C_8H_{17}@SBA\text{-}1$ and $Al(O\mathit{i}Pr)_x@SiMe_2C_8H_{17}@SBA\text{-}1$. The fids were multiplied with an exponential window function increasing the line-width by 10 Hz to reduce noise prior to Fourier transformation. ^{13}C NMR chemical shifts were referred to adamantane. Nitrogen adsorption–desorption isotherms were measured with an ASAP 2020 volumetric adsorption apparatus (Micromeritics) at 77.4 K for relative pressures from 10^{-2} to 0.99 [$a_m(N_2, 77\,K)$) 0.162 nm^2]. Prior to analysis, the samples were outgassed in the degas port of the adsorption analyzer at 523 K for 3 h. The BET specific surface area was obtained from the nitrogen adsorption data in the relative pressure range from 0.04 to 0.20. The pore-size distributions were derived from the desorption branch using the Barrett–Joyner–Halenda (BJH) method.[41] Elemental analyses were performed on an Elementar VarioEL/Perkin-Elmer instrument. The surface silanol population was obtained from the surface coverage $\alpha(SiR_3)$ of activated silylated samples as described previously.[35]

Mesoporous silicas and organosilicas

SBA-1: Surfactant (octadecyltriethylammonium bromide, C_{18}TEABr: 5.0 g, 11.5 mmol), concentrated HCl (37%, 318 g, 2.8 mol), and distilled water (525 g, 29.2 mol) were combined and the resulting mixture was vigorously stirred until a homogeneous solution formed. The solution was cooled to 0 °C and TEOS (12.0 g, 57.6 mmol) was slowly added. Stirring was continued for 4 h, then the reaction mixture was heated in a polypropylene bottle from 0 to 100 °C, and kept at this temperature for 1 h without stirring. The solid product was recovered by filtration (without washing) and dried at ambient temperature. The as-synthesized material was calcined at 540 °C (air, 5 h) and dehydrated in vacuo (270 °C, 10^{-4} Torr, 4 h). The molar composition of the synthesis gel was 1 C_{18}TEABr : 5 TEOS : 280 HCl : 3500 H_2O.

SBA-2: Tetramethylammonium hydroxide (10.0 g, 27.4 mmol, 25 wt% in water) and $C_{16\text{-}3\text{-}1}$ (1.0 g, 2.7 mmol) were dissolved in water (140.0 g, 7.8 mol) and the mixture was stirred until a clear solution was formed (ca. 30 min). TEOS (11.4 g, 54.9 mmol) was added over a period of 5 min and the resulting synthesis mixture was stirred at 25 °C for 2 h. The material was recovered by filtration, washed several times with distilled water, dried overnight in air at ambient temperature, calcined at 540 °C, and finally dehydrated in vacuo (270 °C, 10^{-4} Torr, 4 h). The molar composition of the synthesis gel was 1 $C_{16\text{-}3\text{-}1}$: 20 TEOS : 10 TMAOH : 3000 H_2O.

SBA-16: Pluronic F127 copolymer ($EO_{106}PO_{70}EO_{106}$, 3.0 g) and hydrochloric acid (22.1 g, 37%, 223.8 mmol) were dissolved in distilled water

(117.0 g, 6.5 mol). The solution was warmed to 35 °C, TEOS (11.7 g, 56.0 mmol) was added and the resulting mixture was stirred for about 15 min at this temperature. The mixture was treated for 24 h under static conditions at 35 °C and then heated to 100 °C and kept at this temperature for 24 h. The mesoporous silica was recovered by filtration without washing, dried overnight in air at ambient temperature and then calcined at 540 °C. The molar composition of the synthesis gel was 0.004 Pluronic F127 : 1 TEOS : 4 HCl : 130 H_2O.

PMO[SBA-1]: A mixture of C_{18}TABr (5.84 g, 14.58 mmol), $C_{18\text{-}3\text{-}1}$ (4.24 g, 7.59 mmol), NaOH (3.78 g, 94.50 mmol), and warm deionized water (334 g, 18.6 mol) was stirred for 1 h to form a clear solution. Then 1,2-bis(triethoxysilyl)ethane (BTEE, 14.64 g, 40.05 mmol) was added. Stirring the resulting solution for 24 h at 25 °C and subsequent heating at 95 °C for 6 h brought about precipitation. The final suspension was aged at 95 °C for 24 h. The warm precipitate was recovered by suction filtration without water washing. The molar composition of the synthesis gel was 0.36 C_{18}TABr : 0.19 $C_{18\text{-}3\text{-}1}$: 40.05 BTEE : 2.36 NaOH : 464 H_2O.

The surfactant was removed by a two-step procedure. The as-synthesized mesoporous organosilica (2.0 g) was stirred in ethanol (250 mL) and hydrochloric acid (37 %, 10 g) solution at 50–60 °C for 6 h, and afterwards the solid separated by suction filtration and dried in air. Then the surfactant was further extracted in hydrochloride-acidified ethanol solution for 24 h by using the Soxhlet technique. A weight loss of about 35–45 % was found after a complete solvent extraction. Elemental analysis for the dehydrated solvent-extracted PMO[SBA-1]: C: 16.51, H: 3.39, N: <0.01.

Silylated hybrid materials

General procedure for the synthesis of alkyl dimethylsilylated hybrid materials: In a glovebox, mesoporous silica (SBA-1: 4.01 mmol OH groups per g, SBA-16: 3.03 mmol OH groups per g, calculated from carbon analysis of completely dimethylsilylated materials) was suspended in hexane and a hexane solution of the alkyl dimethyl(dimethylamido)silane (0.30 equivalents relative to surface Si–OH groups) was added. The mixture was stirred at ambient temperature overnight, washed several times with hexane, and dried under vacuum until constant weight.

$SiMe_2C_8H_{17}$@SBA-1: SBA-1 (157 mg) and dimethyl(dimethylamido)octylsilane (40 mg, 0.19 mmol) yielded 168 mg of $SiMe_2C_8H_{17}$@SBA-1.

$SiMe_2C_{18}H_{37}$@SBA-1: SBA-1 (250 mg) and dimethyl(dimethylamido)octadecylsilane (100 mg, 0.28 mmol) yielded 249 mg of $SiMe_2C_{18}H_{37}$@SBA-1.

$SiMe_2C_8H_{17}$@SBA-16: SBA-16 (300 mg) and dimethyl(dimethylamido)octylsilane (58 mg, 0.27 mmol) yielded 284 mg of $SiMe_2C_8H_{17}$@SBA-16.

$SiMe_2C_{18}H_{37}$@SBA-16: SBA-16 (300 mg) and dimethyl(dimethylamido)octadecylsilane (96 mg, 0.27 mmol) yielded 343 mg of $SiMe_2C_{18}H_{37}$@SBA-16.

$SiMe_2C_8H_{17}$@Aerosil300: Aerosil300 (300 mg) and dimethyl(dimethylamido)octylsilane (16 mg, 0.07 mmol) yielded 298 mg of $SiMe_2C_8H_{17}$@Aerosil300.

$SiMe_2C_{18}H_{37}$@Aerosi300: Aerosil300 (300 mg) and dimethyl(dimethylamido)octadecylsilane (26 mg, 0.07 mmol) yielded 265 mg of $SiMe_2C_{18}H_{37}$@Aerosil300.

Aluminated hybrid materials

General procedure for the synthesis of aluminated hybrid materials: In an argon-filled glovebox, the mesoporous silica or organosilica, the mesoporous hybrid material, Aerosil380 or Aerosil300 were suspended in hexane and excess of triethylaluminum was added. The mixture was stirred at ambient temperature overnight, thoroughly washed with hexane to remove unreacted triethylaluminum, and dried under vacuum until constant weight.

$AlEt_x$@SBA-1: SBA-1 (150 mg) and triethylaluminum (100 mg, 0.88 mmol) yielded 214 mg of $AlEt_x$@SBA-1.

$AlEt_x$@$SiMe_2C_8H_{17}$@SBA-1: $SiMe_2C_8H_{17}$@SBA-1 (150 mg) and triethylaluminum (100 mg, 0.88 mmol) yielded 124 mg of $AlEt_x$@$SiMe_2C_8H_{17}$@SBA-1.

$AlEt_x$@$SiMe_2C_{18}H_{37}$@SBA-1: $SiMe_2C_{18}H_{37}$@SBA-1 (200 mg) and triethylaluminum (100 mg, 0.88 mmol) yielded 195 mg of $AlEt_x$@$SiMe_2C_{18}H_{37}$@SBA-1.

$AlEt_x$@PMO[SBA-1]: Following the procedure described above, PMO-[SBA-1] (600 mg) and triethylaluminum (164 mg, 1.44 mmol) yielded 632 mg of $AlEt_x$@PMO[SBA-1].

$AlEt_x$@$SiMe_2C_8H_{17}$@SBA-16: $SiMe_2C_8$@SBA-16 (125 mg) and triethylaluminum (0.69 mg, 0.60 mmol) yielded 136 mg of $AlEt_x$@$SiMe_2C_8H_{17}$@SBA-16.

$AlEt_x$@$SiMe_2C_{18}H_{37}$@SBA-16: $SiMe_2C_{18}H_{37}$@SBA-16 (125) mg and triethylaluminum (69 mg, 0.60 mmol) yielded 128 mg of $AlEt_x$@$SiMe_2C_{18}H_{37}$@SBA-16.

$AlEt_x$@SBA-2: SBA-2 (374 mg) and triethylaluminum (205 mg, 1.79 mmol) yielded 372 mg of $AlEt_x$@SBA-2.

$AlEt_x$@Aerosil380: Aerosil380 (300 mg) and triethylaluminum (200 mg, 1.76 mmol) yielded 311 mg of $AlEt_x$@Aerosil380.

$AlEt_x$@$SiMe_2C_8H_{17}$@Aerosil300: $SiMe_2C_8H_{17}$@Aerosil300 (280 mg) and triethylaluminum (28 mg, 0.24 mmol) yielded 294 mg of $AlEt_x$@$SiMe_2C_8H_{17}$@Aerosil300.

$AlEt_x$@$SiMe_2C_{18}H_{37}$@Aerosil300: $SiMe_2C_{18}H_{37}$@Aerosil300 (250 mg) and triethylaluminum (28 mg, 0.24 mmol) yielded 233 mg of $AlEt_x$@$SiMe_2C_{18}H_{37}$@Aerosil300.

MPV reductions

Reactions were conducted at ambient temperature under an argon atmosphere in a magnetically stirred flask. The flask was charged with anhydrous 2-propanol (4 mL), toluene (1.3 mL), benzaldehyde (66 mg, 0.625 mmol), 1-pyrenecarboxaldehyde (144 mg, 0.625 mmol), and the catalyst (the amount of catalyst was adjusted to 6.6×10^{-2} mmol Al). Samples were taken periodically and analysed by GC, with dodecane as internal standard. Products were identified by NMR spectroscopy.

Acknowledgements

The authors thank the Universitetet i Bergen (program NANOSCIENCE@UiB), the Deutsche Forschungsgemeinschaft, and the Fonds der Chemischen Industrie for support.

[1] M. E. Davis, *Nature* **2002**, *417*, 813–821.
[2] C. T. Kresge, M. E. Leonowicz, W. J. Roth, J. C. Vartuli, J. S. Beck, *Nature* **1992**, *359*, 710–712.
[3] S. Inagaki, S. Guan, T. Ohsuna, O. Terasaki, *Nature* **2002**, *416*, 304–307.
[4] P. Yang, D. Zhao, D. I. Margolese, B. F. Chmelka, G. D. Stucky, *Nature* **1998**, *396*, 152–155.
[5] C. W. Jones, K. Tsuji, M. E. Davis, *Nature* **1998**, *393*, 52–54.
[6] P. B. Weisz, V. J. Frilette, *J. Phys. Chem.* **1960**, *64*, 382–383.
[7] D. L. Wu, A. P. Wight, M. E. Davis, *Chem. Commun.* **2003**, 758–759.
[8] K. Lourvanij, G. L. Rorrer, *Appl. Catal. A* **1994**, 109, 147–165.
[9] O. M. Yaghi, G. Li, H. Li, *Nature* **1995**, *378*, 703–706.
[10] A. M. Pivovar, K. T. Holman, M. D. Ward, *Chem. Mater.* **2001**, *13*, 3018–3031.
[11] M. R. Kishan, N. Srinivas, K. V. Raghavan, S. J. Kulkarni, J. A. R. P. Sarma, M. A. Vairamani, *Chem. Commun.*, **2001**, 2226–2227.
[12] a) Q. Tang, Y. Xu, D. Wu, Y. Sun, *Chem. Lett.* **2006**, 474–475; b) F. Qu, G. Zhu, H. Lin, J. Sun, D. Zhang, S. Li, S. Qiu, *Eur. J. Inorg. Chem.* **2006**, 3943–3947.
[13] J. Aburto, M. Ayala, I. Bustos-Jaimes, C. Montiel, E. Terres, J. M. Dominguez, E. Torres, *Microporous Mesoporous Mater.* **2005**, *83*, 193–200.
[14] C. F. de Graauw, J. A. Peters, H. van Bekkum, J. Huskens, *Synthesis* **1994**, 1007–1017.
[15] E. J. Creyghton, R. S. Downing, *J. Mol. Catal. A* **1998**, *134*, 47–61.
[16] D. Zhao, J. Feng, Q. Huo, N. Melosh, G. H. Frederickson, B. F. Chmelka, G. D. Stucky, *Science* **1998**, *279*, 548–552.
[17] Q. Huo, D. I. Margolese, G. D. Stucky, *Chem. Mater.* **1996**, *8*, 1147–1160.

[18] Q. Huo, R. Leon, P. M. Petroff, G. D. Stucky, *Science* **1995**, *268*, 1324–1327.
[19] D. Zhao, Q. Huo, J. Feng, B. F. Chmelka, G. D. Stucky, *J. Am. Chem. Soc.* **1998**, *120*, 6024–6036.
[20] Y. Sakamoto, M. Kaneda, O. Terasaki, D. Zhao, J. M. Kim, G. Stucky, H. J. Shin, R. Ryoo, *Nature* **2000**, *408*, 449–453.
[21] T.-W. Kim, R. Ryoo, M. Kruk, K. P. Gierszal, M. Jaroniec, S. Kamiya, O. Terasaki, *J. Phys. Chem. B* **2004**, *108*, 11480–11489.
[22] A. E. Garcia-Bennett, S. Williamson, P. A. Wright, I. J. Shannon, *J. Mater. Chem.* **2002**, *12*, 3533–3540.
[23] C. Zapilko, R. Anwander, *Chem. Mater.* **2006**, *18*, 1479–1482.
[24] W. Zhou, H. M. A. Hunter, P. A. Wright, Q. Ge, J. M. Thomas, *J. Phys. Chem. B* **1998**, *102*, 6933–6936.
[25] M. Kaneda, T. Tsubakiyama, A. Carlsson, Y. Sakamoto, T. Ohsuna, O. Terasaki, S. H. Joo, R. Ryoo, *J. Phys. Chem. B* **2002**, *106*, 1256–1266.
[26] M. Perez-Mendoza, J. Gonzalez, P. A. Wright, N. A. Seaton, *Langmuir* **2004**, *20*, 7653–7658.
[27] L. Xin, A. D. Satterfield, J. S. Johnson, *J. Am. Chem. Soc.* **2006**, *128*, 9302–9303.
[28] J. L. Namy, J. Souppe, J. Collin, H. B. Kagan, *J. Org. Chem.* **198**4, 49, 2045–2049.
[29] N. Takezawa, H. Kobayashi, *Chem. Lett.* **1977**, 123–126.
[30] J. R. Ruiz, C. Jimenez-Sanchidrian, J. M. Hidalgo, J. M. Marinas, *J. Mol. Catal. A* **2006**, *246*, 190–194.
[31] R. Anwander, G. Gerstberger, C. Palm, O. Groeger, G. Engelhardt, *Chem. Commun.* **1998**, 1811–1812.
[32] M. J. Kim, R. Ryoo, *Chem. Mater.* **1999**, *11*, 487–491.
[33] Y. Liang, M. Hanzlik, R. Anwander, *J. Mater. Chem.* **2006**, *16*, 1238–1253.
[34] The synthesis of alkyldimethyl(dimethylamido)silanes was performed by reacting lithium dimethylamide $LiN(CH_3)_2$ with the alkyldimethylchlorosilane in tetrahydrofuran solution.
[35] R. Anwander, I. Nagl, M. Widenmeyer, G. Engelhardt, O. Groeger, C. Palm, T. Roeser, *J. Phys. Chem. B* **2000**, *104*, 3532–3544.
[36] M. Kruk, V. Antochshuk, J. R. Matos, L. P. Mercuri, M. Jaroniec, *J. Am. Chem. Soc.* **2002**, *124*, 768–769.
[37] H. Schlaad, A. H. E. Müller, *Macromol. Rapid Commun.* **1994**, *15*, 517–525.
[38] A. Abraham, R. Prins, J. A. van Bokhoven, E. R. H. van Eck, A. P. M. Kentgens, *J. Phys. Chem. B* **2006**, *110*, 6553.
[39] R. Anwander, C. Palm, O. Groeger G. Engelhardt, *Organometallics* **1998**, *17*, 2027–2036.
[40] R. Zana, M. Benrraou, R. Rueff, *Langmuir* **1991**, *7*, 1072.
[41] E. P. Barrett, L. G. Joyner, P. P. Halenda, *J. Am. Chem. Soc.* **1951**, *73*, 373–380.

Received: November 9, 2006
Published online: January 4, 2007

